RSC Advances

PAPER

View Article Online
View Journal | View Issue

Cite this: *RSC Adv.*, 2024, **14**, 38815

Decomplexation of Pb-EDTA by electron beam irradiation technology: efficiency and mechanism†

Mengxin Tu,‡[a] Lei Chen,‡[ac] Jianzhong Gu,*[ac] Chengkai Mao,[a] Yingfei Ren,[a] Hongyong Wang[a] and Gang Xu*[abc]

Received 10th July 2024
Accepted 7th October 2024

DOI: 10.1039/d4ra04993d

rsc.li/rsc-advances

As a common heavy metal complex in industrial wastewater, Pb-EDTA has garnered much attention due to its detrimental impact on both human health and the ecological environment. The degradation of heavy metal complexes by traditional methods requires subsequent treatment to recover heavy metals. This article attempts to find an effective method to simultaneously degrade both organic matter and heavy metal pollutants. Experimental results indicate that 1 mM Pb-EDTA can be effectively removed at 10 kGy with a degradation efficiency of 91.62%. Most lead ions were still in a stable complex state, with a removal rate of 24.42% (10 kGy). When the absorbed dose increased to 80 kGy, the degradation efficiency of Pb-EDTA was 95.24%. At this time, the removal rate of Pb^{2+} reached 68.82%. Through radical scavenging experiments and further mechanism analysis, it was demonstrated that electron beam irradiation primarily generates ·OH radicals, disrupting the structure of Pb-EDTA, gradually decarboxylating, and ultimately generating formic acid, acetic acid, and NO_3^-. The released metal ions were reduced by e_{aq}^- and ·H to obtain lead monomers. Residual toxicity analysis indicates that the toxicity of degradation products generated by electron beam irradiation is significantly reduced. Experimental results showed that electron beam irradiation can effectively degrade Pb-EDTA and recover lead ions simultaneously.

1. Introduction

With the continuous development of industrial production, sectors like electroplating and metal smelting generate and discharge a large amount of heavy metal wastewater every year.[1] Due to concerns for human health and the ecological environment, heavy metal pollution has grown to be a significant issue today.[2] One of the most pervasive heavy metal contaminants is lead (Pb), primarily generated through smelting, mining, coal burning, waste incineration, and leaded gasoline production.[3] Lead is a toxic heavy metal that can be inhaled and ingested from a variety of places, including contaminated food, water, soil, and air. Compared with lead alone, synthetic chelating agents like ethylenediamine tetraacetate (EDTA) can create robust complexes with Pb^{2+}, which are more stable and complex.[4] As a potent hexadentate chelating ligand, EDTA is mostly utilized in pharmacy, textiles, papermaking, household detergents, and industrial cleaning.[5] Even though EDTA is not toxic to mammals at ambient levels, concerns have been raised that it may facilitate the transfer of toxic heavy metals from sewage sludge and sediments since EDTA can reactivate adsorbed or precipitated metal ions.[4,5]

To degrade these heavy metal complexes with high mobility, a number of treatment techniques have been developed such as adsorption,[6] chemical precipitation,[7] and ion exchange.[8] However, because of the persistent solubility characteristics of metal complexes, these conventional processes often fail to achieve the desired degradation.[9,10] Due to the great oxidizing ability, advanced oxidation processes (AOPs) have developed as effective chemical oxidation technologies for the degradation of heavy metal complexes.[11] The reaction mechanism of advanced oxidation technology is a process that generates ·OH through different techniques,[12] including Fenton oxidation,[13,14] electrochemical oxidation,[15] photocatalytic oxidation,[16,17] and ozone oxidation.[18] Once ·OH is formed in the system, the organic matter in the water body is attacked by a series of chain reactions, degrading it to H_2O, CO_2, or inorganic salts, *etc.*[19] There have been some studies using AOPs to degrade Pb-EDTA. Vohra *et al.* (2000)[20] showed that UV/TiO_2 was effective in removing Pb-EDTA complexes from water. Finžgar *et al.* (2006)[21] used ozone/UV to treat heavy metal complexes in soil extractants with actual removal rates of 49.6% for Pb and 19.9% for Zn during the

[a]*School of Environmental and Chemical Engineering, Shanghai University, 99 Shangda Road, Shanghai 200444, PR China. E-mail: jzhgu@staff.shu.edu.cn; xugang@shu.edu.cn; Fax: +86 21 6998 2749; +86 21 66137787; Tel: +86 21 6998 2744; +86 21 66138250*

[b]*Key Laboratory of Organic Compound Pollution Control Engineering, Ministry of Education, Shanghai, 200444, PR China*

[c]*Shanghai, University, Shanghai Institute Applied Radiation, 20 Chengzhong Road, Shanghai 200444, PR China*

† Electronic supplementary information (ESI) available. See DOI: https://doi.org/10.1039/d4ra04993d

‡ Mengxin Tu and Lei Chen contributed equally to this article.

degradation of Pb-EDTA and Zn-EDTA, respectively. However, according to Zhao *et al.* (2014),[22] photocatalytic oxidation can be limited by the rapid compounding of pairs of electron holes and the low use of visible light. Low oxidation efficiency can also be caused by the selectivity and limited solubility of ozone in water.[23] In addition, the degradation products of heavy metal complexes treated with AOPs require further alkali treatment and other means to recover the heavy metals. Therefore, with the aim to address the problems that still exist with the present AOPs, it is urgently necessary to further investigate and explore alternative procedures for the degradation of heavy metal–organic complexes.[24]

Electron Beam (EB) irradiation is a technology that uses high-energy radiation to generate active products such as oxidizing radicals and reducing radicals from water irradiation without changing the radioactivity of the solution, as shown in eqn (1).[25,26]

$$H_2O \rightarrow 2.7\cdot OH + 2.6e_{aq}^- + 0.6H\cdot + 2.6H_3O^+ + 0.45H_2 + 0.7H_2O_2 \quad (1)$$

The numbers in the formula indicate the values of the radiochemical yield (the so-called *G*-value) in a pure neutral aqueous solution, which was defined as the number of product molecules formed (or initial molecules changed) for every 100 eV of energy absorbed.[27] The most important advantage of using EB irradiation is the highly effective *in situ* generation of the extremely reactive oxidation radical ·OH and unique strong reductive hydrated electrons by water radiolysis, which can achieve advanced oxidation and reduction processes (AO/RP) simultaneously.[28] However, there has been limited research on the influencing factors, degradation mechanisms and pathways, and the toxicity of degradation products of EB irradiation.

This study focused on Pb-EDTA as the representative metal complex to study the influencing factors and mechanism of EB irradiation degradation. The experiment explored the impacts of absorbed dose, initial concentration, solution pH, and the co-existing substances in actual environments on degradation efficiency. The main active radicals in the reaction system were determined, the degradation byproducts were analyzed and the possible degradation pathways for Pb-EDTA were proposed. Furthermore, a quantitative structure–activity relationship (QSAR) was used to evaluate the toxicity of Pb-EDTA degradation products.

2. Experimental section

2.1. Chemical reagents

Lead chloride ($PbCl_2$) and ethylenediaminetetraacetic acid disodium salt dihydrate (Na_2EDTA) were purchased from Sinopharm Chemical Reagent Co., Ltd (China). Solutions of Pb-EDTA were prepared by mixing a solution of $PbCl_2$ and Na_2-EDTA to obtain a 1 : 1 molar ratio of Pb^{2+}/EDTA. Analytical grade hydrogen peroxide, potassium persulfate, and formic acid for use as oxidizers were purchased from Merck and Sigma-Aldrich (China).

Analytical grade sodium carbonate, sodium bicarbonate, sodium sulfate, sodium sulfite, nitrite, and sodium nitrite were purchased from Chemical Reagent Shanghai Co., Ltd (China), as anion production reagents. The pH of solutions was adjusted to the desired value by using HCl or NaOH. Since Pb-EDTA was obtained by mixing $PbCl_2$ and Na_2EDTA, a high concentration of Cl^- was present in the solution itself, so the amount of Cl^- introduced during pH adjustment using hydrochloric acid could be almost negligible. Deionized water was used for the preparation and dilution of solutions.

2.2. Irradiation experiment procedure

The Pb-EDTA degradation experiments were conducted with an electron accelerator (GJ-2-II, Xianfeng Electrical Company) supplied by the Institute of Applied Radiation, Shanghai University, China. The beam energy of the device was 1.8 MeV and the variable current was 0–10 mA. Before irradiation, the prepared Pb-EDTA solution was uniformly encapsulated in plastic bags with a volume and thickness of 20 mL and 2 mm, respectively. If required, the samples were purged with high-purity gas (N_2 or O_2) for half an hour before irradiation. The packaged sample was irradiated by the electron accelerator, with two sets of irradiation doses. One group was set at 4, 6, 8, and 10 kGy, which was a low radiation dose group. The other group was set at 50, 60, 80, 100, and 120 kGy, which was a high radiation dose group. The 10 mL Fricke dosimeter solution samples were stored in 40 mL, 1–2 mm thick polyethylene bags at room temperature (20 ± 2 °C). We placed the Fricke dosimeter and Pb-EDTA solutions under the same conditions for simultaneous irradiation to measure the absorbed dose of the Pb-EDTA solutions. Since the thickness of the irradiation bags was only 1–2 mm, the effect on the penetration of the electron beam was almost non-existent, and therefore the loss of the electron beam irradiation dose was negligible. After irradiation, each sample was centrifuged at 12 000 rpm for 15 min and then filtered through a 0.45 μm aqueous polytetrafluoron (PTFE) syringe filter for analysis. All of the experiments were carried out in three sets of parallel experimental measurements.

The remaining metal complexes Pb EDTA, Pb, and total organic carbon content in the irradiated solution were analyzed and detected, and the removal efficiency of each indicator was calculated by eqn (2).

$$\text{Removal efficiency} = \frac{C_0 - C_D}{C_0} \times 100\% \quad (2)$$

C_0: the initial content of metal complexes, metal ions, and TOC. C_D: the residual content of metal complexes, metal ions, and TOC.

2.3. Analytical methods

The concentration of Pb-EDTA was measured by high-performance liquid chromatography (HPLC, Agilent 1260) equipped with a C18 column (250 mm × 4.6 mm × 5 μm). The sample was analyzed with an injection volume of 20 μL. The isocratic elution was comprised of 80% formate buffer (15 mM formic acid, 5 mM sodium formate, and 1 mM TBA-Br) and 20%

acetonitrile (v/v) at a temperature of 25 °C. The flow rate was set as 1 mL min^{-1} and the detection wavelength was 254 nm.[9]

Atomic Absorption Spectrometry (AA, Agilent 280FS) was utilized to quantify the lead ions concentration. Using acetylene as the fuel gas, the detection wavelength is set at 217.0 nm, with a lamp current of 10 mA. The flame composition is air/acetylene, maintained at an airflow rate of 13.5 L min^{-1} and an acetylene flow rate of 2.00 L min^{-1}. The concentration measurement range spans from 0 to 20 mg L^{-1}.

The mineralization of Pb-EDTA was evaluated by total organic carbon (TOC) concentration, which was estimated by multi N/C 3100 TOC analyzer (Analytik Jena AG Corporation, Germany).

The distribution of Pb-EDTA species as a function of pH was obtained from the Visual MINTEQ 3.0 software.

The intermediates of Pb-EDTA were identified by HPLC (Agilent 1260) coupled with quadrupole time of flight mass spectrometry (Q-TOF-MS, Agilent 6545) in full-scan mode.

Formic acid, acetic acid, oxalic acid, glycolic acid, and NO_3^- were detected by ion chromatography (IC, ICS-6000, Thermo Scientific) with a conductivity detector.

After Pb-EDTA complexation, the precipitates were collected by pumping and filtering, and dried in a vacuum freeze drier. The crystalline structure of the precipitate was characterized by X-ray diffraction analysis (XRD, D/max 2550 V, Rigaku) with Cu Kα radiation at a 2θ scanning rate of 8° min^{-1} (40 kV, 25 mA).

2.4. Toxicity assessment

The software toxicity evaluation software (T.E.S.T.) was applied to calculate the growth inhibition, bioaccumulation factors (BAF), developmental toxicity, and acute toxicity of Pb-EDTA and its degradation intermediates, which was based on quantitative structure–activity relationship (QSAR) models.

3. Results and discussion

3.1 Effect of the initial concentration of Pb-EDTA

To determine the degradation efficiency of Pb-EDTA at varied concentrations, we set up a variety of concentration gradients (0.25, 0.5, 0.75, and 1 mM) in the irradiation experiment with absorbed doses of 4, 6, 8, and 10 kGy. As shown in Fig. 1a, Pb-EDTA was effectively degraded at low absorbed doses, indicating that EB irradiation can degrade heavy metal complexes. The pseudo second order kinetic model can be fitted to describe the decomposition of Pb-EDTA, as indicated in eqn (3):[29]

$$\frac{1}{C} - \frac{1}{C_0} = kD \quad (3)$$

where k represents the pseudo second order rate constant, and D represents the absorbed dose of EB irradiation. As observed in Fig. 1a, the value of k decreased with the increase of Pb-EDTA concentration, indicating that the metal complex degraded more readily when its initial concentration was lower. The primary cause of this phenomenon is that as the absorbed dose increases, more intermediates are generated during the degradation of Pb-EDTA at high concentrations, and these intermediates also react with active radicals to reduce their concentration.[30] As shown in Fig. 1c, under the low irradiation dose group, Pb^{2+} was not effectively removed, and the highest removal rate of Pb^{2+} was only 24.42% (10 kGy).

To achieve synchronous removal of heavy metal ions, we further increased the absorbed dose to 50, 60, 80, 100, and 120 kGy. As shown in Fig. 1b, Pb-EDTA was almost completely removed. Fig. 1d shows that at a specific Pb-EDTA concentration, the removal rate of Pb^{2+} increased first and then decreased as the EB irradiation absorbed dose increased. With the absorbed dose was 80 kGy and the starting concentration was 1 mM, the removal rate of Pb^{2+} was 68.82%. By the time the absorbed dose reached 120 kGy, the removal rate of Pb^{2+} dropped to 65.40%.

This is because when the irradiation dose is low, the concentration of reactive radicals is also low, and the interaction between radicals is negligible, whereas with the gradual increase of irradiation dose, the concentration of reactive radicals increases, and the interactions between radicals are more intense, as shown in eqn (4)–(7),[31,32] which reduces the effective concentration of reactive radicals, thus affecting the degradation rate of Pb-EDTA and the removal rate of Pb^{2+}. To clarify the precipitate generated in the solution after irradiation, we characterized it through XRD, and the results proved that the precipitate was the lead elemental precipitate obtained after the reduction of Pb^{2+}. We will discuss this in detail in Section 3.5 identification of degradation intermediates. To investigate the simultaneous removal of the complex and Pb^{2+}, the removal rate of Pb^{2+} was more suitable for assessing the efficiency of the EB irradiation degradation.

$$\cdot OH + \cdot OH \rightarrow H_2O_2\, k = 5.5 \times 10^9\ M^{-1}\ s^{-1} \quad (4)$$

$$\cdot H + \cdot OH \rightarrow H_2O\, k = 7.0 \times 10^9\ M^{-1}\ s^{-1} \quad (5)$$

$$e_{aq}^- + \cdot OH \rightarrow OH^-\, k = 3.0 \times 10^{10}\ M^{-1}\ s^{-1} \quad (6)$$

$$H_2O + \cdot H + e_{aq}^- \rightarrow H_2 + OH^-\, k = 2.5 \times 10^{10}\ M^{-1}\ s^{-1} \quad (7)$$

Besides the pollutant removal efficiency, the mineralization rate can also be used to assess the degradation effect of EB irradiation.[33] To illustrate that the TOC values detected after irradiation did not affected by the degradation of the irradiated bags, we used pure water for comparison with blank irradiation at 50–120 kGy, and the results, shown in Fig. S1,† showed that with increasing irradiation dose, only very low TOC was detected in the pure water, which was negligible. Fig. 1e demonstrates the TOC removal of Pb-EDTA at different concentrations and absorbed doses. It is apparent that the mineralization rate of the complexes continuously rises when the absorbed dose increases. This is mainly because of the rise in absorbed dosage, which causes ·OH to oxidize and break down more intermediate products. The results demonstrate that EB irradiation is a successful technique for pollutant degradation, achieving efficient removal of pollutants and the reduction and precipitation of heavy metals.

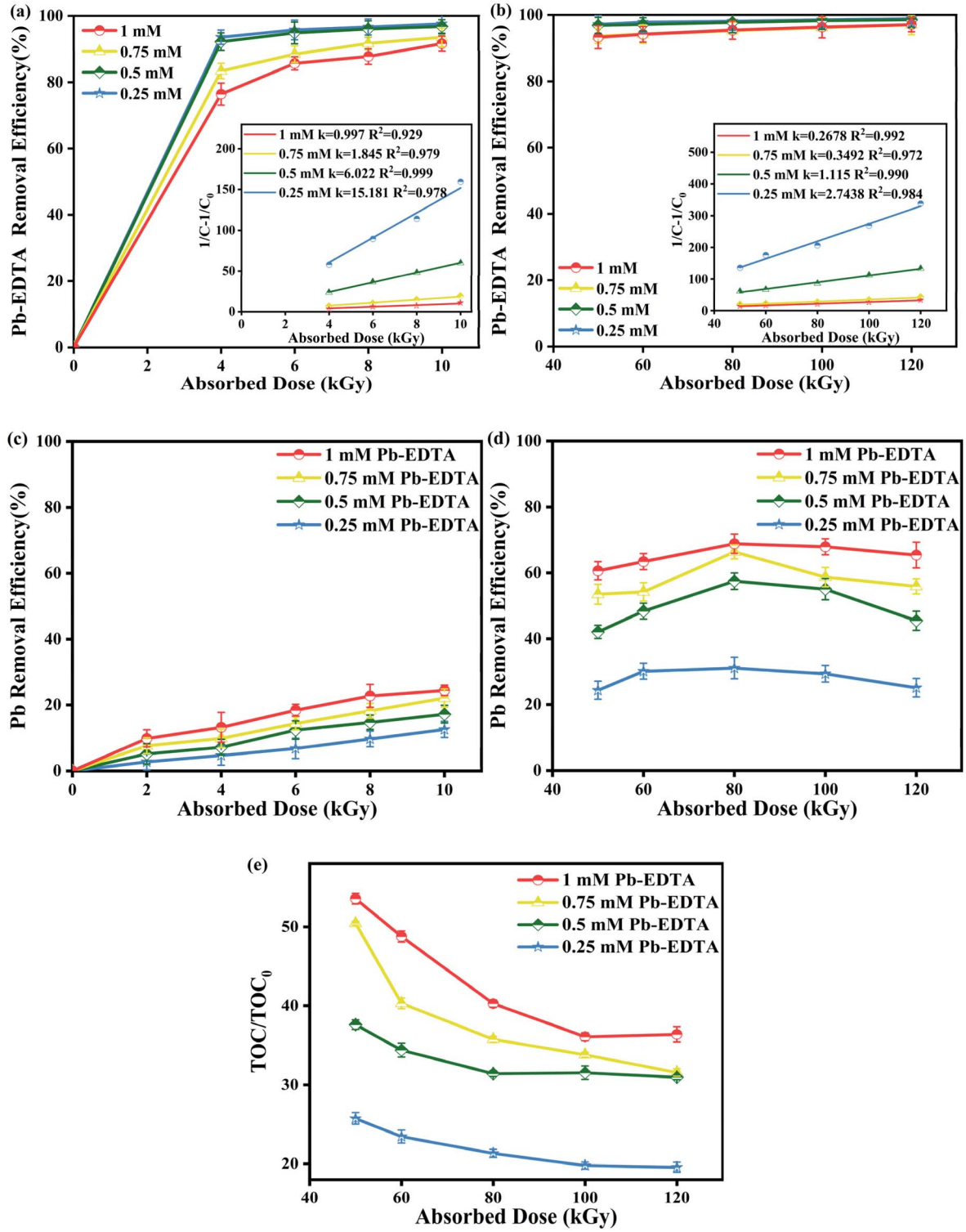

Fig. 1 (a) The impact of initial concentration on Pb-EDTA degradation under the low dose group; (b) the impact of initial concentration on Pb-EDTA degradation under the high dose group; (c) the impact of initial concentration on Pb^{2+} removal under the low dose group; (d) the impact of initial concentration on Pb^{2+} removal under the high dose group; (e) the impact of initial concentration on TOC removal.

3.2. Effect of the initial pH of Pb-EDTA

The existence form of the heavy metal complexes in the water body changes with the change of pH. The distribution of Pb-EDTA complex morphology and its content change in the pH range of 0–14 were simulated by Visual MINTEQ software, as shown in Fig. 2a. Pb-EDTA is stable over a wide range of pH conditions and mainly exists in the form of $PbEDTA^{-2}$. Only under acidic conditions at pH 3, Pb-EDTA is protonated into

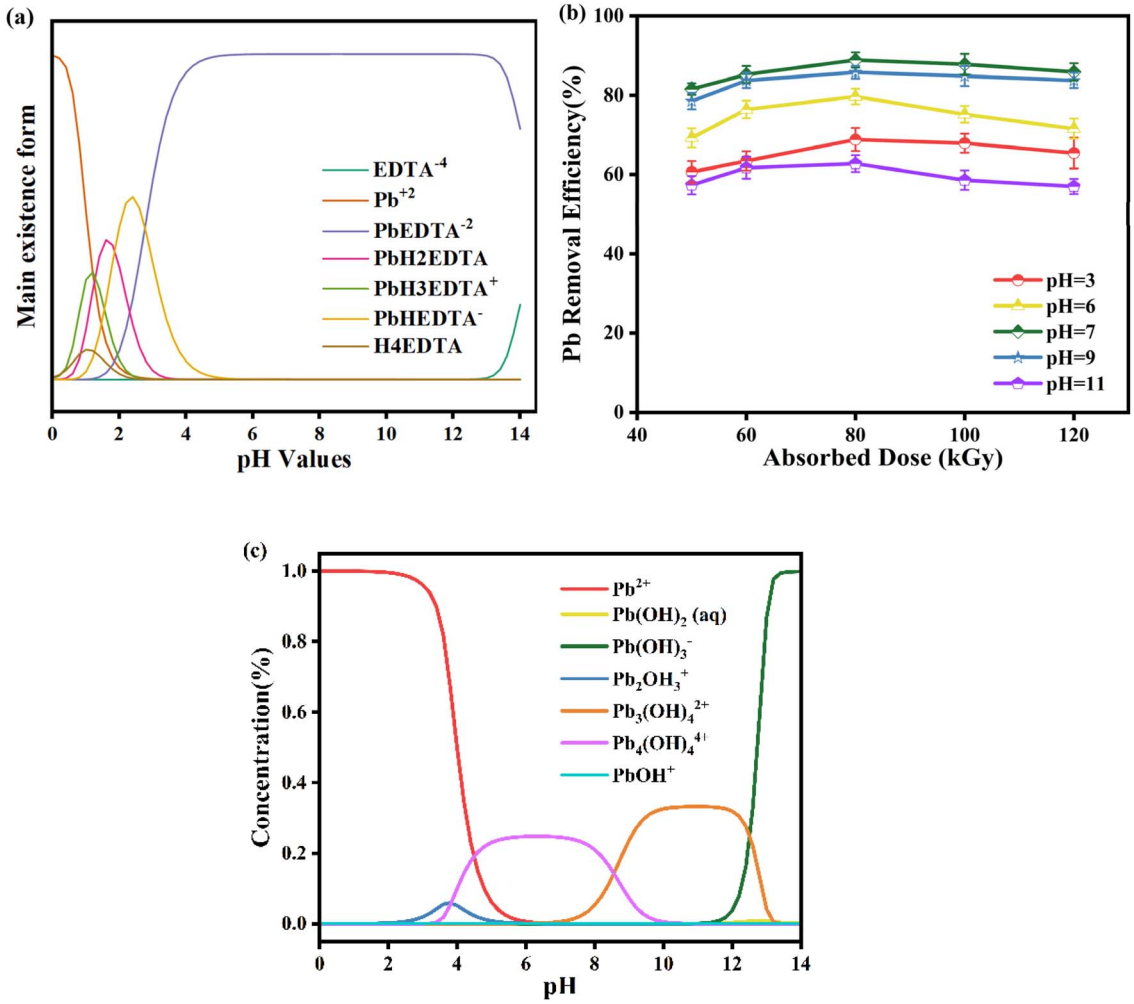

Fig. 2 (a) The different forms of Pb-EDTA at various pH values; (b) the impact of initial pH on Pb^{2+} removal; (c) the different forms of lead ions at various pH values.

$PbHEDTA^{-}$ and PbH_2EDTA^{-}, which are more prone to react with ·OH than $PbEDTA^{-2}$. Generally speaking, protonated species are more susceptible to the attack of reactive free radicals than deprotonated species, so acidic conditions are favorable for the removal of Pb-EDTA. The removal rate of Pb^{2+} through the irradiation degradation of Pb-EDTA at pH 3, 6, 7, 9, and 11 was shown in Fig. 2b. We selected a concentration of 1 mM for Pb-EDTA in our experiment, which is similar to the concentration of pollutants in the actual environment, ensuring that the experiment can accurately reflect the removal of Pb-EDTA in water bodies. The results indicated that the efficiency of Pb^{2+} removal initially increased and then decreased with varying pH levels in the solution. At an absorbed dose of 80 kGy, the Pb^{2+} removal rate was 68.82% at pH 3. The removal of Pb^{2+} was more effective when the solution pH was adjusted to neutral, reaching a peak rate of 88.85% at pH 7 (80 kGy). However, as the pH level continued to rise to 11, the Pb^{2+} removal rate dropped to a minimum of 62.74% (80 kGy). This indicates that the removal of Pb^{2+} is not only influenced by the initial morphology of Pb-EDTA, but also attributed to two reasons: (1) under the over-acidic condition, e_{aq}^{-} generated by EB irradiation reacts with hydrogen ions, making it fail to reduce Pb^{2+}, as shown in eqn (8).[34] The research results are based on earlier studies, as shown in Fig. S2,† where the G value of active radicals generated by EB irradiation changes with pH values. Under alkaline conditions, the reduction of Pb^{2+} removal rate could be owing to the lower yield of ·OH produced by EB irradiation hydrolysis and the reaction between hydroxyl radicals and hydroxide ions, as shown in eqn (9),[35] the degree of reaction between radicals and complexes weakens and thus the removal efficiency is reduced.[27] (2) Studies have shown that lead ions exist in different forms at different pH values,[36] as seen in Fig. 2c. Under acidic conditions, the main form of lead ions is Pb^{2+}, and when under alkaline conditions, they mainly exist in the form of $Pb(OH)_3^{-}$. In general, the present state of Pb^{2+} tends to deprotonate as the pH of the solution increases. Compared to deprotonated species, protonated species are more susceptible to attack by reactive radicals, so alkaline conditions are unfavorable for Pb^{2+} removal compared to acidic conditions.

$$e_{aq}^{-} + H^{+} \rightarrow \cdot H \; k = 2.3 \times 10^{10}\ M^{-1}\ s^{-1} \quad (8)$$

$$OH^{-} + \cdot OH \rightarrow \cdot O^{-} \; k = 1.2 \times 10^{10}\ M^{-1}\ s^{-1} \quad (9)$$

3.3 Effect of reactive species

The effect of reactive radicals generated during irradiation on the removal of Pb-EDTA was determined by adding different types of quenching agents to the solution. O_2 can react with e_{aq}^- and H· (eqn (10) and (11)).[37] Therefore, when the solution is purged with O_2, ·OH plays a predominant role in the degradation of Pb-EDTA. When N_2 is introduced into the solution, it does not affect the activity of various types of free radicals. This is mainly because N_2 is an inert gas used only to degas the solution. The activity of reactive free radicals varies under different pH conditions. When the solution pH is greater than 3, the contribution of H· is minimal. In this case, the primary reactive species here are e_{aq}^- and ·OH. However, when the pH of the solution is less than 3, the contribution of e_{aq}^- is minimal. In this instance, the primary active ingredients are H· and ·OH.[38] *Tert*-Butanol (TBA) was added separately under the two pH conditions. Since TBA is an effective burster of ·OH (eqn (12)),[39] at this time, H· dominates in solutions with a pH above 3, in removing pollutants.

$$O_2 + e_{aq}^- \rightarrow O_2^{\bullet -}\ k = 9.1 \times 10^{10}\ M^{-1}\ s^{-1} \quad (10)$$

$$O_2 + H^{\cdot} \rightarrow HO_2^{\cdot}\ k = 2.1 \times 10^{10}\ M^{-1}\ s^{-1} \quad (11)$$

$$(CH_3)_3COH + \cdot OH \rightarrow (CH_3)_2C(\cdot CH_2)OH + H_2O\ k = 1.9 \times 10^{10}\ M^{-1}\ s^{-1} \quad (12)$$

$$Cl^- + OH\cdot \rightarrow ClOH^{\bullet -}\ 4.3 \times 10^9\ M^{-1}\ s^{-1} \quad (13)$$

$$ClOH^{\bullet -} \rightarrow Cl^- + OH\cdot\ 6.1 \times 10^9\ M^{-1}\ s^{-1} \quad (14)$$

The impact of different reactive radicals on the removal rate of Pb^{2+} is displayed in Fig. 3. Compared with the initial group, the reduction efficiency of Pb^{2+} decreased slightly under O_2 purification, and ·OH predominated in the degradation of pollutants. After adding TBA, when H· and e_{aq}^- were the main free radicals, Pb^{2+} reduction efficiency significantly decreased. This indicates that the removal of ·OH prevents Pb-EDTA from being oxidatively degraded, and Pb^{2+} is not effectively released from the metal-complex ligand, thus hindering its reduction and removal.

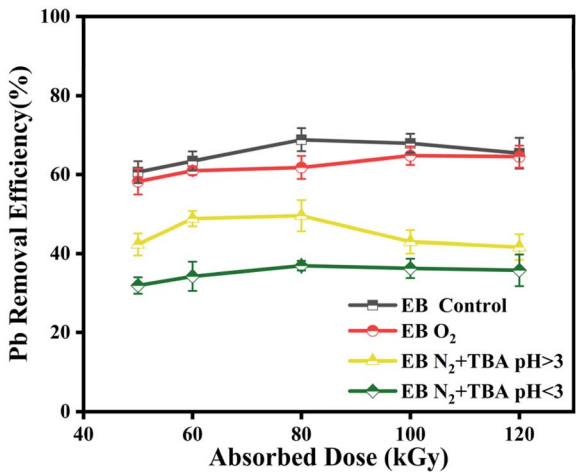

Fig. 3 The impact of different active radicals on Pb^{2+} removal.

Since the experimental solution was prepared by mixing $PbCl_2$ and Na_2EDTA, this result also suggests that the presence of Cl^- and the interreaction with hydroxyl radicals (eqn (13) and (14))[40] do not scavenge hydroxyl radicals from the system. Therefore, it can be inferred that the electron beam irradiation technique for Pb-EDTA removal is influenced by various active free radicals, primarily the ·OH radicals, which can disrupt the structure of Pb-EDTA, enabling the stepwise decarboxylation and simultaneous generation of low molecular weight compounds. Subsequently, the released metal ions are reduced by e_{aq}^- and H· radicals.

3.4 Identification of degradation intermediates

The majority of the pertinent research suggests that metal-EDTA degrades through a similar process in which the complex is progressively decarboxylated by reactive radicals attacking the C–N bond of the ligand.[41–43] To investigate the degradation pathway of Pb-EDTA in the EB irradiation process, the degradation by-products were analyzed using a liquid-phase mass spectrometer and an ion chromatography analytical instrument. Table S1† shows the degradation intermediates of Pb-EDTA formed in EB irradiation. As reported in other literature,[9,44] Pb-ED3A (m/z = 437.3748), Pb-ED2A (m/z = 381.3546), NTA (m/z = 191.139), and IMDA (m/z = 133.1027) were the major degradation products during the EB irradiation reaction. Analysis of small molecule acids using ion chromatography revealed that formic acid, acetic acid, and NO_3^- were mainly present in the irradiated solution. Fig. 4a shows that all these small molecule acids gradually increased with increasing absorbed doses. Significant precipitates could be found in the samples after EB irradiation, which were characterized by XRD to further determine the composition and nature of the precipitates. As shown in Fig. 4b, the precipitated phase shows obvious diffraction peaks of Pb monoclinic crystal structure at 2θ values of 31.4°, 36.3°, 52.3°, 62.2°, 65.4°, 85.6°, and 88.2°. Fig. S3† shows the SEM image of the precipitated product.

Based on the relevant references and detected degradation intermediates and degradation products,[45] the possible degradation pathways of Pb-EDTA during the EB irradiation reaction were proposed, as shown in Fig. 5. Two possible degradation pathways were hypothesized to exist. First, ·OH attacks the C–N bond of Pb-EDTA, causing it to break and split into Pb-ED3A and CH_3COOH; then continues to attack the carboxyl site of Pb-ED3A and subsequently forms Pb-ED2A. In the degradation pathway II, the reactive radicals act on the C–N bond to generate NTA and IMDA. Finally, the generated intermediates are further oxidized to small organic acids and inorganic ions including formic acid, acetic acid, and NO_3^-. The released Pb^{2+} is reduced to lead monomers by the reducing radicals. In summary, similar to previous studies, the degradation of Pb-EDTA by EB irradiation is mainly achieved by attacking the complex with active radicals and gradually decarboxylating it.

3.5 Comparison of EB, EB/H_2O_2, EB/$K_2S_2O_8$, EB/HCOOH process

EB irradiation technology can be combined with different oxidants and reductants to affect the degradation efficiency of

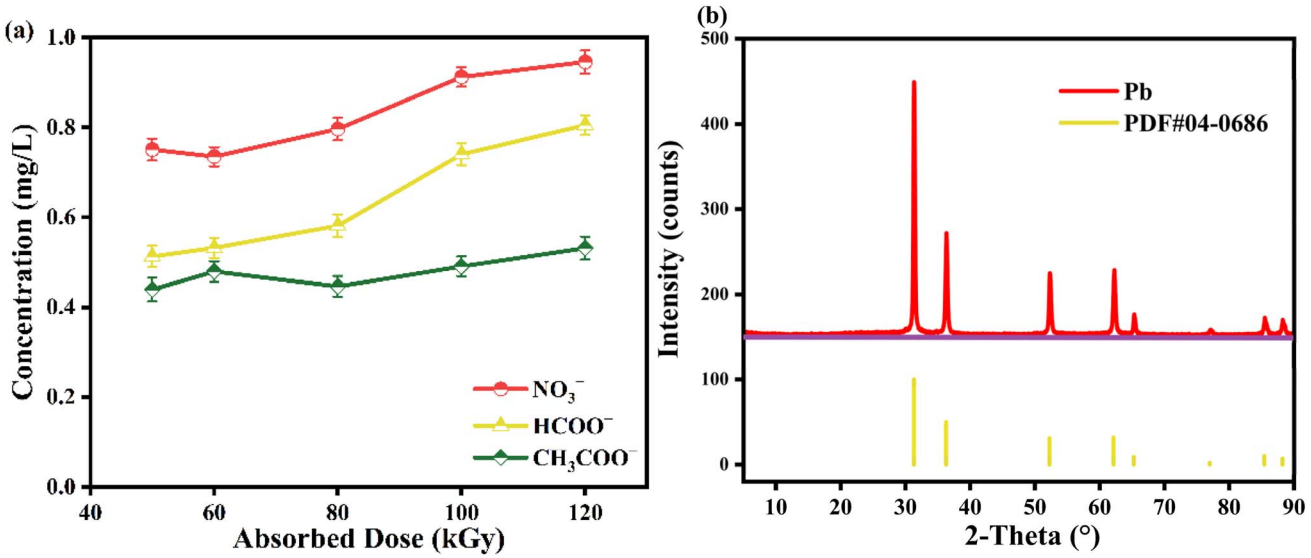

Fig. 4 (a) The content of formic acid, acetic acid, and nitric acid; (b) XRD of precipitates.

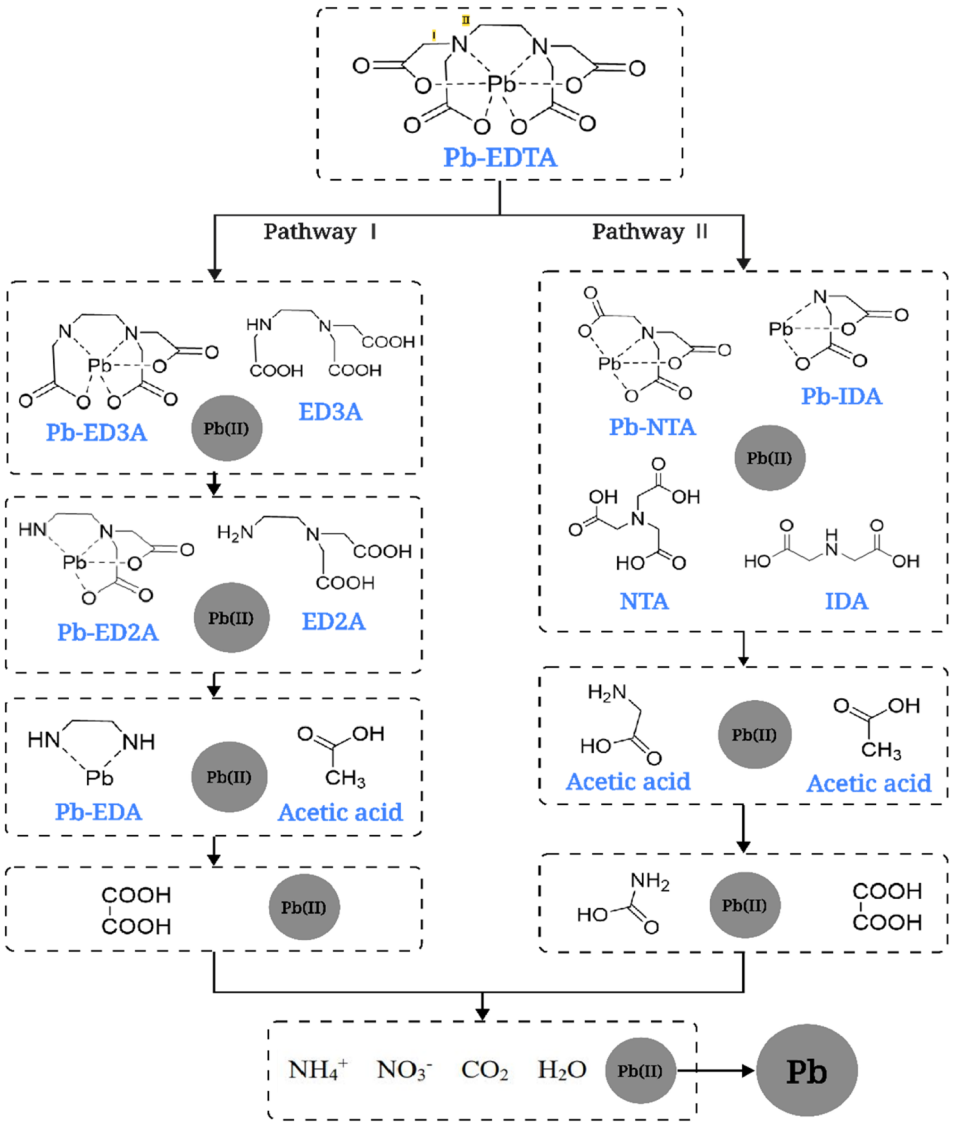

Fig. 5 Possible degradation pathways of Pb-EDTA.

Pb-EDTA. In our experiments, we investigated the impact of oxidants hydrogen peroxide (H_2O_2),[46] potassium persulfate ($K_2S_2O_8$),[47] and the reductant formic acid (HCOOH)[48] on the removal rate of Pb^{2+}. To have an appropriate comparison of the effect of just the additives, we adjusted the solution pH to a constant value (pH 7) by adding NaOH after adding different oxidizing/reducing agent concentrations.

3.5.1 Removal rate of Pb^{2+} in EB/H_2O_2 process. Fig. 6a displays the removal rate of Pb^{2+} through EB irradiation degradation of Pb-EDTA after adding 5, 10, and 20 mM H_2O_2. At 80 kGy, when the concentration of H_2O_2 increased to 20 mM, the highest removal rate reached 93.97%. This is mainly because when H_2O_2 concentration increases, it is conducive to developing oxidizing active free radical ·OH (eqn (15) and (16)),[49] which is conducive to the removal of Pb-EDTA.

$$e_{aq}^- + H_2O_2 \rightarrow \cdot OH + OH^- \; k = 1.1 \times 10^9\ M^{-1}\ s^{-1} \quad (15)$$

$$H\cdot + H_2O_2 \rightarrow \cdot OH + H_2O \; k = 9.0 \times 10^7\ M^{-1}\ s^{-1} \quad (16)$$

3.5.2 Removal rate of Pb^{2+} in EB/$K_2S_2O_8$ process. Fig. 6b illustrates the removal rate of Pb^{2+} through EB irradiation degradation of Pb-EDTA after adding 5, 10, and 20 mM $K_2S_2O_8$, respectively. The highest removal rate of Pb^{2+} reached 98.60% after adding 20 mM $K_2S_2O_8$ (80 kGy). It indicates that the addition of $K_2S_2O_8$ to the system improved the removal rate of Pb^{2+}. This is the result of the rapid reaction of $S_2O_8^{2-}$ with ·H and e_{aq}^- converted to reactive $\cdot SO_4^-$ (eqn (17) and (18)).[37] Because of its high redox potential (E_0 = 2.73 V), $\cdot SO_4^-$ is regarded as a potent one-electron oxidant akin to ·OH (E_0 = 2.60 V).[50] Some studies have indicated that $\cdot SO_4^-$ could react with $S_2O_8^{2-}$ to form a reductive free radical (eqn (19)).[51]

$$S_2O_8^{2-} + H\cdot \rightarrow \cdot SO_4^- + H^+ + SO_4^{2-} \; k = 2.5 \times 10^7\ M^{-1}\ s^{-1} \quad (17)$$

$$S_2O_8^{2-} + e_{aq}^- \rightarrow \cdot SO_4^- + SO_4^{2-} \; k = 1.1 \times 10^{10}\ M^{-1}\ s^{-1} \quad (18)$$

$$\cdot SO_4^- + S_2O_8^{2-} \rightarrow S_2O_8^{\cdot -} + SO_4^{2-} \; k = 1.2 \times 10^6\ M^{-1}\ s^{-1} \quad (19)$$

3.5.3 Removal rate of Pb^{2+} in EB/HCOOH process. Fig. 6c displays the removal rate of Pb^{2+} through EB irradiation degradation of Pb-EDTA after adding 5, 10, and 20 mM HCOOH. Compared to the previous two oxidants, adding 10 mM HCOOH at 80 kGy resulted in a removal rate of only 76.01% for Pb^{2+}. When the concentration of HCOOH was raised to 20 mM, the removal rate of Pb^{2+} decreased to 62.87% (80 kGy). This phenomenon is caused by the fact that $HCOO^-$ can react with ·OH (eqn (20)).[52] Therefore, low concentrations of $HCOO^-$ promote the reductive precipitation of Pb^{2+}, whereas when $HCOO^-$ is added at too high a dosage, too many reducing species are produced in the system, inhibiting the generation of oxidizing radicals, which negatively affects the generation of reducing species converted from oxidizing species, leading to a significant inhibition of Pb^{2+} removal.

$$\cdot OH + HCOO^- \rightarrow \cdot CO_2^- + H_2O \; k = 3.2 \times 10^9\ M^{-1}\ s^{-1} \quad (20)$$

Meanwhile, to better illustrate the influence of the dose-effect on the removal efficiency, supplementary experiments were conducted on the removal efficiency of Pb^{2+} with different additive contents at low doses, and the results are shown in Fig. S4.†

3.6 Effects of common co-existing substances in real water bodies

For the common components in industrial wastewater, we select natural organic matter and inorganic anions to study the impact of coexisting substances on Pb-EDTA degradation in the EB irradiation process.[53,54]

3.6.1 Effect of humic acid. As shown in Fig. 7a, the addition of a certain amount of humic acid can significantly enhance the precipitation of Pb^{2+}. This is because humic acid itself can act as an electron medium or electron donor, excite the triple excited state of HA ($^3HA^*$), and generate a substantial amount of reactive oxidation radicals like ·OH, single molecule oxygen, and H_2O_2, further contributing to the removal efficiency.[54,55] According to studies, humic acid contains a large amount of inorganic ions, which can also promote the precipitation of Pb^{2+}.

3.6.2 Effect of coexisting ions. Since common inorganic anions are present in real water, their coexistence in water significantly affects the reaction process, as they may influence

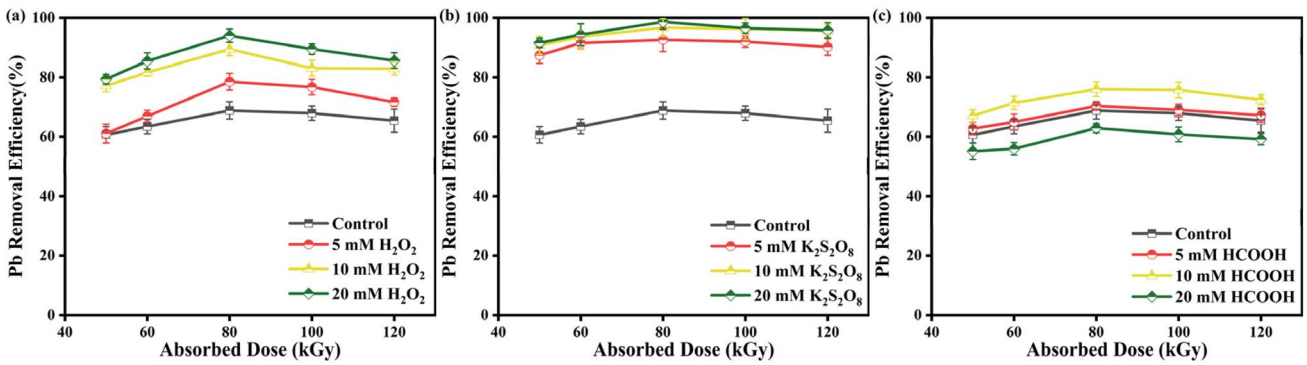

Fig. 6 (a) The impact of H_2O_2 dosage on Pb^{2+} removal; (b) the impact of $K_2S_2O_8$ dosage on Pb^{2+} removal; (c) the impact of HCOOH dosage on Pb^{2+} removal.

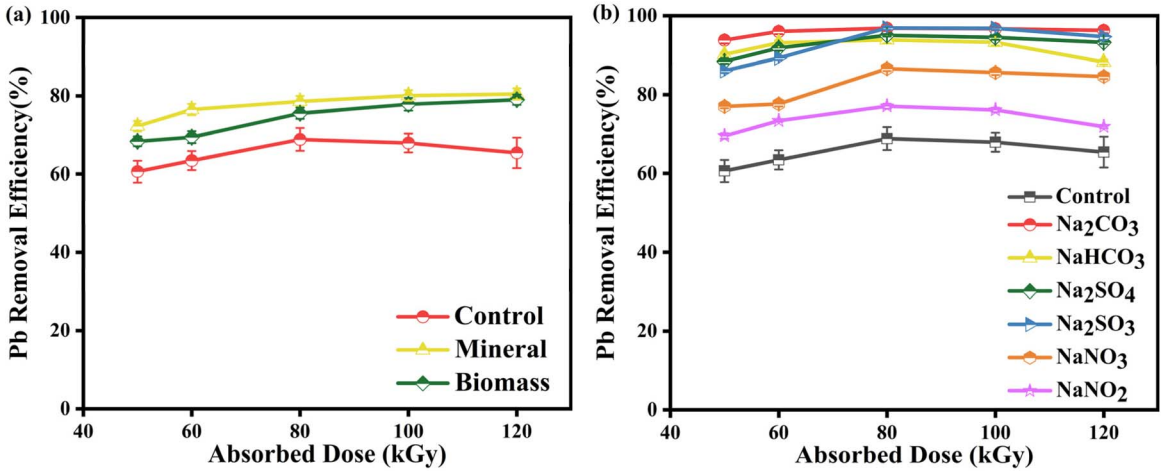

Fig. 7 (a) The impact of humic acid on Pb^{2+} removal; (b) the impact of coexisting ions on Pb^{2+} removal.

the reactions of Pb-EDTA with the reactive radicals generated during irradiation. In this study, these anions (CO_3^{2-}, HCO_3^-, NO_3^-, NO_2^-, SO_4^{2-}, and SO_3^{2-}) were selected (all with a concentration of 10 mM) and added to the Pb-EDTA solution to be irradiated.[56] As displayed in Fig. 7b, the addition of various anions enhanced the removal rate of Pb^{2+} to varying degrees compared to the control group.

When CO_3^{2-} or HCO_3^- is introduced, they react with ·OH and e_{aq}^- to produce $CO_3^{\cdot-}$ (eqn (21)–(25)),[57] with CO_3^{2-} and HCO_3^- having significantly higher reaction rates with ·OH than with e_{aq}^-, resulting in the reduction of ·OH in the EB system,[58] which thereby inhibiting the degradation of Pb-EDTA. However, on the other hand, CO_3^{2-} reacts with ·OH to form $CO_3^{\cdot-}$ also has some ability to oxidatively degrade metal complexes, and compared with ·OH, $CO_3^{\cdot-}$ has a lower redox potential (1.59 V), so the free lead ions released by irradiation degradation will not be re-oxidized due to the strong oxidizing atmosphere in the system, which is more conducive to the removal of lead ions by reduction.

$$HCO_3^- + e_{aq}^- \rightarrow HCO_3^{2-}\ k = 6.0 \times 10^5\ M^{-1}\ s^{-1} \quad (21)$$

$$HCO_3- + \cdot OH \rightarrow CO_3^{\cdot-} + H_2O\ k = 8.5 \times 10^6\ M^{-1}\ s^{-1} \quad (22)$$

$$HCO_3^- + H\cdot \rightarrow CO_3^{\cdot-} + H_2\ k = 4.0 \times 10^4\ M^{-1}\ s^{-1} \quad (23)$$

$$CO_3^{2-} + e_{aq}^- \rightarrow CO_3^{3-}\ k = 3.9 \times 10^5\ M^{-1}\ s^{-1} \quad (24)$$

$$CO_3^{2-} + \cdot OH \rightarrow CO_3^{\cdot-} + OH^-\ k = 3.9 \times 10^8\ M^{-1}\ s^{-1} \quad (25)$$

The addition of SO_4^{2-} promoted the degradation of Pb-EDTA. This is mainly because SO_4^{2-} can combine with ·OH to generate highly oxidative compounds $\cdot SO_4^-$ (eqn (26)).[40] $\cdot SO_4^-$, as an additional oxidizing substance, can cooperate with the oxidizing radicals generated by electron beam irradiation and jointly attack the organic ligand structure, thus enhancing the removal efficiency of the system for Pb-EDTA. When SO_3^{2-} is added, it interacts with ·OH to generate $\cdot SO_3^-$ (eqn (27)), leading to the removal of excess ·OH in the system, thus freeing the de-complexed lead ions from the strong oxidizing atmosphere in the system and making it more conducive to the reductive removal by reducing radicals.

$$SO_4^{2-} + \cdot OH \rightarrow \cdot SO_4^- + OH^-\ k = 6.5 \times 10^7\ M^{-1}\ s^{-1} \quad (26)$$

$$SO_3^{2-} + \cdot OH \rightarrow \cdot SO_3^- + OH^-\ k = 5.5 \times 10^9\ M^{-1}\ s^{-1} \quad (27)$$

The addition of NO_3^- or NO_2^- promotes the reduction and removal of Pb^{2+} to a certain extent. This is because NO_3^- and NO_2^- easily react with ·OH, e_{aq}^- and ·H to generate $\cdot NO_3^-$ and $\cdot NO_2^-$ (eqn (28)–(35)),[59] with oxidation-reduction potentials of 1.03 V and 0.94 V, respectively. This is much lower than the active potential of free radicals that originally existed in the system, leading to an increase in the reducing atmosphere in the system and further promoting the reduction and removal of Pb^{2+}.

$$NO_3^- + e_{aq}^- \rightarrow NO_3^{\cdot 2-}\ k = 9.7 \times 10^9\ M^{-1}\ s^{-1} \quad (28)$$

$$NO_3^- + H^{\cdot} \rightarrow NO_2^{\cdot} + OH^-\ k = 4.4 \times 10^6\ M^{-1}\ s^{-1} \quad (29)$$

$$NO_3^- + H^+ \rightarrow HNO_3\ k = (4.4\text{–}6.0) \times 10^8\ M^{-1}\ s^{-1} \quad (30)$$

$$HNO_3 + \cdot OH \rightarrow NO_3^{\cdot-} + H_2O\ k = (0.88\text{–}1.2) \times 10^8\ M^{-1}\ s^{-1} \quad (31)$$

$$NO_2^- + \cdot OH \rightarrow NO_2^{\cdot} + OH^-\ k = 6.0 \times 10^9\ M^{-1}\ s^{-1} \quad (32)$$

$$NO_2^- + \cdot OH \rightarrow HNO_3\ k = 1.0 \times 10^{10}\ M^{-1}\ s^{-1} \quad (33)$$

$$NO_2^- + H\cdot \rightarrow NO + OH^-\ k = 7.1 \times 10^8\ M^{-1}\ s^{-1} \quad (34)$$

$$NO_2^- + e_{aq}^- \rightarrow NO_3^{\cdot 2-}\ k = 3.5 \times 10^9\ M^{-1}\ s^{-1} \quad (35)$$

Furthermore, inorganic ions such as carbonate and sulfate have higher reaction rates with free radicals, but compared to nitrate and nitrite ions, their presence significantly improves the removal efficiency of Pb^{2+}. We speculate that Pb^{2+} released

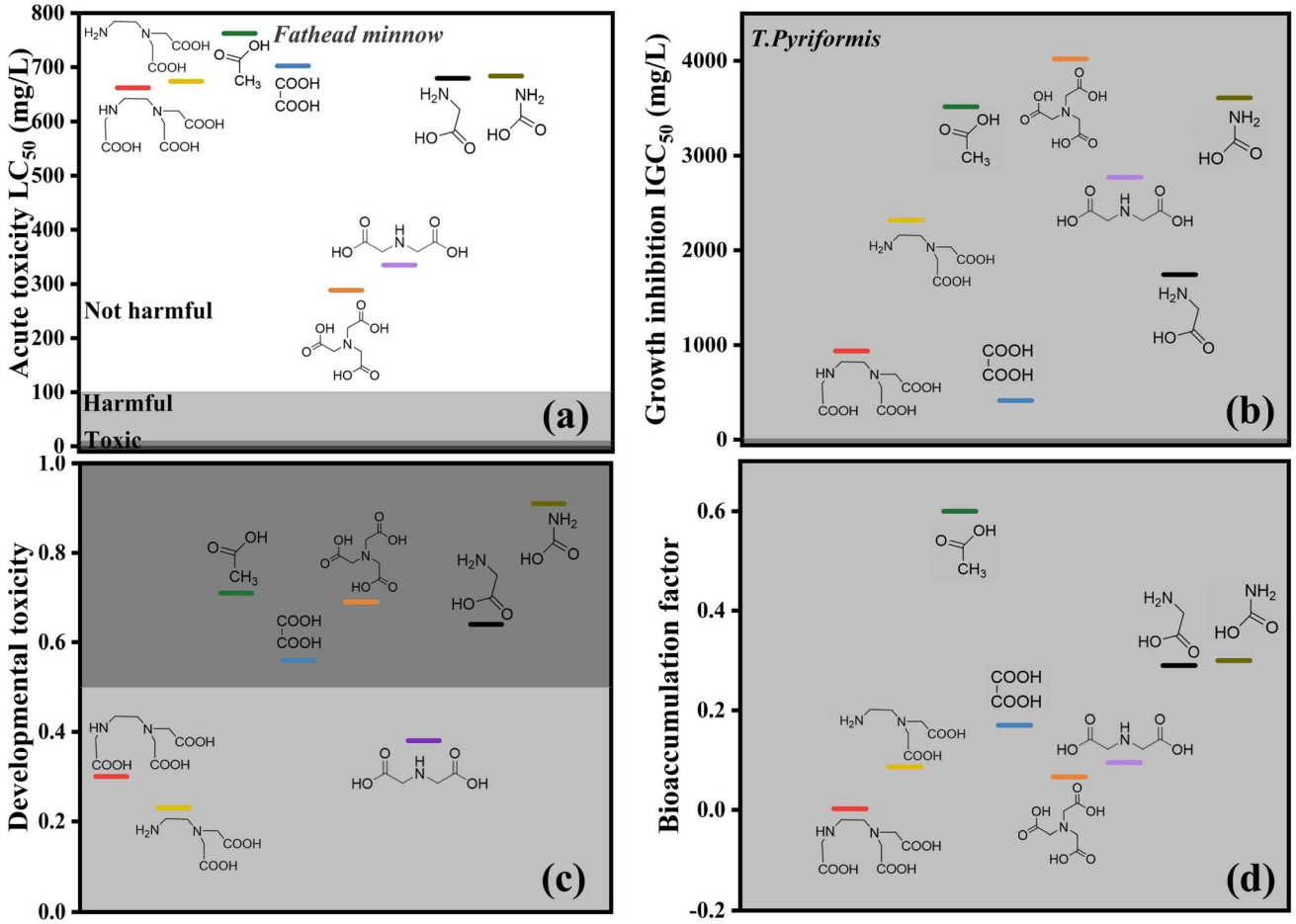

Fig. 8 Toxicity calculation of Pb-EDTA degradation intermediates generated during EB irradiation: (a) acute oral rat LD_{50}; (b) growth inhibitory concentration of Tetrahymena pyriformis IGC_{50}; (c) developmental toxicity; (d) bioaccumulation factor.

by the degradation of Pb-EDTA would be precipitated through reactions with inorganic anions, in addition to being reduced directly to Pb monomer. This speculation might be supported by the white precipitate observed in the irradiation bag after irradiation of the solution.

3.7 Residual toxicity analysis

Considering the experimental cost, the toxicity of degradation intermediates was assessed in advance by theoretical calculations to verify the potential toxicity of irradiation-treated solutions. Ecological structure activity relationship (ECOSAR) is a computerized prediction system for toxicity in aquatic systems developed by the US Environmental Protection Agency (US EPA). The system uses mathematical models of example training sets of a range of chemicals to predict chemicals that may cause long-term effects. The model's prediction of toxicity for compounds to be tested presupposes that these compounds to be tested are sufficiently similar to those in the training set. Therefore, in the present study, the toxicity calculation software T.E.S.T (Version 5.1) based on Quantitative Constitutive Effect Relationship (QSAR) modeling was adopted to calculate the toxicity of Pb-EDTA and its degradation intermediates. Acute toxicity LC_{50}, growth inhibition IGC_{50}, developmental toxicity, and bioaccumulation factor (BAF) were selected. By comparing the toxic effects of EDTA before and after irradiation treatment, the hazardous effects of EB irradiation applied in the treatment of degraded Pb-EDTA on environmental organisms were evaluated.

Fig. 8 shows that the degradation intermediates of Pb-EDTA are less toxic, and ED2A and ED3A both show lower toxicity. Table S2† shows the specific toxicity data of the intermediates. The intermediate product was continually oxidized and degraded as the absorbed dose of EB increased. The toxicity of NTA and IDA was higher than that of ED2A and ED3A, but the toxicity of the final degradation products was far less than that of the intermediate products. As a result, the overall toxicity of the solution was trending downward during the degradation process. According to the total toxicity estimations from this investigation, the degradation of Pb-EDTA was accompanied by the generation of toxic intermediates. The toxic effect of the degradation products created by the EB irradiation was, however, significantly reduced, showing that it was an effective means.

4. Conclusions

In this study, electron beam irradiation was used for the oxidative degradation of Pb-EDTA and the reduction of Pb^{2+} simultaneously. The article explored how various environmental substrates affect electron beam irradiation. The findings show that neutral conditions are favorable to the removal of Pb^{2+}. Compared to other oxidants, $K_2S_2O_8$ and H_2O_2 promoted the oxidative degradation of Pb-EDTA. The reactive radicals in the system were impacted by the addition of a certain amount of humic substances and inorganic ions, which altered the efficiency of the degradation. Experiments on mechanism research revealed that ·OH was the main radical for degradation of Pb-EDTA, and e_{aq}^- mainly reduced lead ions. The degradation pathway of Pb-EDTA was proposed based on the discovered intermediates and degradation products. Factors such as pH, inorganic ions, and natural organic matter can affect the concentration and types of free radicals. During electron beam irradiation, high concentrations of oxidative and reductive free radicals are generated. Oxidative free radicals attack Pb-EDTA, leading to decomplexation, while reductive free radicals interact with lead ions, causing their transformation into elemental lead.

However, it is important to note that Pb-EDTA removal is a complex process, and changes in the oxidizing and reducing properties of the system can both impact the removal of Pb-EDTA. Inorganic ions and organic molecules in the environment can react with free radicals, altering their concentrations and subsequently affecting the removal efficiency of Pb-EDTA. Experimental results have indicated that most environmental factors can inhibit the removal of Pb-EDTA to some extent, highlighting the need for further research on the transformation of free radicals in different environments.

Data availability

The data that support the findings of this study are available from the corresponding author upon reasonable request.

Conflicts of interest

There are no conflicts to declare.

Acknowledgements

The authors thank National Natural Science Foundation of China (No. 12175133, and 12075148). We would also appreciate the Guizhou Provincial Key Technology R&D Program (No. QKHZC-2024-152).

References

1 X. Q. Kan, Y. Q. Dong, L. Feng, M. Zhou and H. B. Hou, *Chemosphere*, 2021, **267**, 128909.
2 S. Huang, L. Gu, N. Zhu, K. Feng, H. Yuan, Z. Lou, Y. Li and A. Shan, *Green Chem.*, 2014, **16**, 2696–2705.
3 F. Y. AlJaberi, *J. Environ. Chem. Eng.*, 2018, **6**, 6069–6078.
4 B. Nowack, F. G. Kari and H. G. Krüger, *Water, Air, Soil Pollut.*, 2001, **125**, 243–257.
5 F. G. Kari and W. Giger, *Water Res.*, 1996, **30**, 122–134.
6 L. Wu, H. Wang, H. Lan, H. Liu and J. Qu, *Sep. Purif. Technol.*, 2013, **117**, 118–123.
7 S. Mauchauffée and E. Meux, *Chemosphere*, 2007, **69**, 763–768.
8 D. Kołodyńska, H. Hubicka and Z. Hubicki, *Desalination*, 2008, **227**, 150–166.
9 X. Huang, Y. Xu, C. Shan, X. Li, W. Zhang and B. Pan, *Chem. Eng. J.*, 2016, **299**, 23–29.
10 J. Rivera-Utrilla, M. Sánchez-Polo, M. Á. Ferro-García, G. Prados-Joya and R. Ocampo-Pérez, *Chemosphere*, 2013, **93**, 1268–1287.
11 C. P. Huang, C. Dong and Z. Tang, *Waste Manage.*, 1993, **13**, 361–377.
12 J. L. Wang and L. J. Xu, *Crit. Rev. Environ. Sci. Technol.*, 2012, **42**, 251–325.
13 P. Bautista, A. F. Mohedano, J. A. Casas, J. A. Zazo and J. J. Rodriguez, *J. Chem. Technol. Biotechnol.*, 2008, **83**, 1323–1338.
14 L. Szabó, T. Tóth, T. Engelhardt, G. Rácz, C. Mohácsi-Farkas, E. Takács and L. Wojnárovits, *Sci. Total Environ.*, 2016, **551–552**, 393–403.
15 C. A. Martinez-Huitle and S. Ferro, *Chem. Soc. Rev.*, 2006, **35**, 1324–1340.
16 X. Huang, X. Wang, D.-X. Guan, H. Zhou, K. Bei, X. Zheng, Z. Jin, Y. Zhang, Q. Wang and M. Zhao, *Environ. Sci. Pollut. Res.*, 2019, **26**, 8516–8524.
17 F. Rehman, M. Sayed, J. A. Khan, N. S. Shah, H. M. Khan and D. D. Dionysiou, *J. Hazard. Mater.*, 2018, **357**, 506–514.
18 J. L. Wang and H. Chen, *Sci. Total Environ.*, 2020, **704**, 135249.
19 A. O. Oluwole, E. O. Omotola and O. S. Olatunji, *BMC Chem.*, 2020, **14**, 62.
20 M. S. Vohra and A. P. Davis, *Water Res.*, 2000, **34**, 952–964.
21 N. Finžgar and D. Leštan, *Chemosphere*, 2006, **63**, 1736–1743.
22 X. Zhao, L. Guo and J. Qu, *Chem. Eng. J.*, 2014, **239**, 53–59.
23 T. E. Agustina, H. M. Ang and V. K. Vareek, *J. Photochem. Photobiol., C*, 2005, **6**, 264–273.
24 M. Trojanowicz, A. Bojanowska-Czajka and A. Capodaglio, *Environ. Sci. Pollut. Res.*, 2017, **24**, 20187–20208.
25 W. Jianlong and W. Jiazhuo, *J. Hazard. Mater.*, 2007, **143**, 2–7.
26 N. K. Vel Leitner, I. Guilbault and B. Legube, *Radiat. Phys. Chem.*, 2003, **67**, 41–49.
27 J. Wang and L. Chu, *Radiat. Phys. Chem.*, 2016, **125**, 56–64.
28 M. Trojanowicz, *Sci. Total Environ.*, 2020, **718**, 134425.
29 T. Li, S. He, L. Kou, J. Peng, H. Liu, W. Zou, Z. Cao and T. Wang, *Sep. Purif. Technol.*, 2023, **306**, 122588.
30 A. A. Basfar, H. M. Khan, A. A. Al-Shahrani and W. J. Cooper, *Water Res.*, 2005, **39**, 2085–2095.
31 K. Lin, W. J. Cooper, M. G. Nickelsen, C. N. Kurucz and T. D. Waite, *Appl. Radiat. Isot.*, 1995, **46**, 1307–1316.
32 B. G. Zheng, Z. Zheng, J. B. Zhang, X. Z. Luo, J. Q. Wang, Q. Liu and L. H. Wang, *Desalination*, 2011, **276**, 379–385.
33 L. J. Xu and J. L. Wang, *Appl. Catal., B*, 2012, **123**, 117–126.

34 Y. Liu, J. Hu and J. Wang, *Environ. Technol.*, 2014, **35**, 2028–2034.
35 Z. Guo, F. Zhou, Y. Zhao, C. Zhang, F. Liu, C. Bao and M. Lin, *Chem. Eng. J.*, 2012, **191**, 256–262.
36 S. He, T. Li, L. Zhang, X. Zhang, Z. Liu, Y. Zhang, J. Wang, H. Jia, T. Wang and L. Zhu, *Chem. Eng. J.*, 2021, **424**, 130515.
37 Z. Huo, S. Wang, H. Shao, H. Wang and G. Xu, *Environ. Sci. Pollut. Res.*, 2020, **27**, 20807–20816.
38 S. Wang, J. Hu, S. He and J. Wang, *J. Hazard. Mater.*, 2022, **433**, 128727.
39 S.-H. Ma, M.-H. Wu, L. Tang, R. Sun, C. Zang, J.-J. Xiang, X.-X. Yang, X. Li and G. Xu, *Nucl. Sci. Tech.*, 2017, **28**, 137.
40 J. Wang and S. Wang, *Chem. Eng. J.*, 2021, **411**, 128392.
41 Y. Cao, X. Qian, Y. Zhang, G. Qu, T. Xia, X. Guo, H. Jia and T. Wang, *Chem. Eng. J.*, 2019, **362**, 487–496.
42 Z. Xu, C. Shan, B. Xie, Y. Liu and B. Pan, *Appl. Catal., B*, 2017, **200**, 439–447.
43 S. Liang, X. Hu, H. Xu, Z. Lei, C. Wei and C. Feng, *Appl. Catal., B*, 2021, **296**, 120375.
44 M. Pan, C. Zhang, J. Wang, J. W. Chew, G. Gao and B. Pan, *Environ. Sci. Technol.*, 2019, **53**, 8342–8351.
45 D. Jiraroj, F. Unob and A. Hagège, *Water Res.*, 2006, **40**, 107–112.
46 N. S. Shah, J. A. Khan, M. Sayed, Z. U. H. Khan, J. Iqbal, S. Arshad, M. Junaid and H. M. Khan, *Sep. Purif. Technol.*, 2020, **233**, 115966.
47 X. Chen and J. Wang, *J. Cleaner Prod.*, 2021, **328**, 129625.
48 Q. Wang, Y. Zhang, Y. Li, J. Ren, G. Qu, T. Wang and H. Jia, *Chem. Eng. J.*, 2022, **427**, 131584.
49 M. S. Alam, M. Kelm, B. S. M. Rao and E. Janata, *Radiat. Phys. Chem.*, 2004, **71**, 1087–1093.
50 J. L. Wang and S. Z. Wang, *Chem. Eng. J.*, 2018, **334**, 1502–1517.
51 J. Criquet and N. K. V. Leitner, *Chemosphere*, 2009, **77**, 194–200.
52 H. Ren, Z. Hou, X. Han and R. Zhou, *Chem. Eng. J.*, 2017, **309**, 638–645.
53 L. Chen, T. Cai, C. Cheng, Z. Xiong and D. Ding, *Chem. Eng. J.*, 2018, **351**, 1137–1146.
54 J. J. Lopez-Penalver, M. Sanchez-Polo, C. V. Gomez-Pacheco and J. Rivera-Utrilla, *J. Chem. Technol. Biotechnol.*, 2010, **85**, 1325–1333.
55 S. L. H. Sandvik, P. Bilski, J. D. Pakulski, C. F. Chignell and R. B. Coffin, *Mar. Chem.*, 2000, **69**, 139–152.
56 N. Liu, W.-Y. Huang, Z.-M. Li, H.-Y. Shao, M.-H. Wu, J.-Q. Lei and L. Tang, *Sep. Purif. Technol.*, 2018, **202**, 259–265.
57 S. Wang and J. Wang, *Chem. Eng. J.*, 2018, **351**, 688–696.
58 N. Liu, T. Wang, M. Zheng, J. Lei, L. Tang, G. Hu, G. Xu and M. Wu, *Chem. Eng. J.*, 2015, **270**, 66–72.
59 H.-Y. Shao, M.-H. Wu, F. Deng, G. Xu, N. Liu, X. Li and L. Tang, *Chemosphere*, 2018, **190**, 184–190.